HYDROCODE MODELLING OF SPACE DEBRIS HYPERVELOCITY IMPACT ON SODA-LIME GLASS USING THE JOHNSON-HOLMQUIST BRITTLE MATERIAL MODEL

Emma A. Taylor[1], Colin J. Hayhurst[2] and Konstantinos Tsembelis[1]

[1] *Unit for Space Sciences and Astrophysics, University of Kent at Canterbury, Canterbury, CT2 7NR, U.K.*
(phone: +44 1227 764000 xt 3834 fax: +44 1227 762616 email: eat1@ukc.ac.uk)
[2] *Century Dynamics Ltd, Dynamics House, Hurst Road, Horsham, Surrey, RH12 2DT, U.K.*

ABSTRACT

We present the initial results of an implementation of the Johnson-Holmquist 2 (JH-2) model within the AUTODYN-2D™ hydrocode using a Lagrangian grid. The code results were compared to the results of a hypervelocity impact (HVI) programme on to soda-lime glass carried out at the Unit for Space Sciences and Astrophysics at the University of Kent. The experimental data (also presented here) cover a velocity range of 4 - 6 km s^{-1} and projectile diameter and density ranges of 800 - 2000 μm and 1 - 8 g cm^{-3} respectively.
An analysis of empirically determined power-law damage equations is also presented, using data from six shot programmes (165 data points). We find that the current damage equations, used to provide hydrocode calibration data for velocities beyond the experimental range, show systematic trends in depth with velocity. The hydrocode modelling results are within the limits of the two power-law penetration equations, although the model does not reproduce spallation diameters as observed on experimental targets. The tentative conclusion is that the Johnson-Holmquist model is applicable to compressive regimes but does not appear to predict tensile fracture.

1. INTRODUCTION

Hydrocodes enable the investigation of impact mass/velocity regimes and time-resolved phenomena not easily accessible in the laboratory. However, the usefulness of any modelling is dependent on the quality and applicability of the material models used (equation of state (EOS), strength and failure models). A range of material models have been developed and validated for ductile (metallic) targets at high strain rates (the ballistic impact regime). Subsequently, these models have been validated for hypervelocity impact on ductile targets. Hypervelocity impact simulations have not, however, been validated for brittle targets, in particular glass. Brittle materials such as glass have been shown to display effects such as dilation and exhibit significant residual strength under compression. These features have been incorporated into the Johnson-Holmquist 2 brittle material model (Ref. 1). We present initial results of hydrocode simulations using the JH-2 model for brittle materials within the AUTODYN-2D™ hydrocode (Ref. 2, Ref. 3). Simulations were run for a 1 mm Al projectile at velocities between 5 and 15 km s^{-1}. Calibration data, also presented here, are provided by the impact programme onto soda-lime glass which was performed at the Light Gas Gun facility (University of Kent at Canterbury). These data, combined with 135 data points from other brittle material hypervelocity tests, are used to assess the predictive ability of current empirical damage equations, as used for calibration beyond the experimental regime.
Flux decoding of space flown solar arrays (Ref. 7) has led to analysis and assessment of glass damage equations (Ref. 8). Codes such as AUTODYN have been validated for hypervelocity impacts onto thick and thin ductile targets (Ref. 4, Ref. 5, Ref. 6). Previous brittle material hydrocode modelling (Ref. 9, Ref. 10, Ref. 11) have used simple models (e.g. the Mohr-Coulomb strength model) to model the damage. The Johnson-Holmquist model gives the yield strength as a function of pressure, includes a damage model, the residual strength in fractured material, dilation and strain rate effects, making it more sophisticated for modelling the material strength of glass under hypervelocity impact.

2. THE JOHNSON-HOLMQUIST 2 MODEL

The Johnson-Holmquist 2 model (Ref. 1) is applicable for brittle materials subjected to large strains, high strain rates and high pressures. It was developed for the ballistic impact regime and is principally a phenomological rather than a theoretical model. The yield strength is a damage (D) based interpolated function of intact and fracture strength (Eq. 1).
The intact strength and fractured strength are represented by Eqs. 2 and 3, where A, N, M, C and B are experimentally determined material constants.

$$\sigma^* = \sigma_i^* - D(\sigma_i^* - \sigma_f^*) \quad (1)$$

$$\sigma_i^* = A(P^* + T^*)^N(1 + C\ln\dot{\varepsilon}^*) \quad (2)$$

$$\sigma_f^* = B(P^*)^M(1 + C\ln\dot{\varepsilon}^*) \quad (3)$$

The normalised stresses (σ^*, σ_f^*, σ_i^*) have the following general form, σ/σ_{HEL}, where σ is the actual equivalent stress and σ_{HEL} is the equivalent stress at the Hugoniot Elastic Limit (HEL), P* is the normalised hydrostatic pressure (P/P_{HEL}) and T* is the normalised maximum tensile hydrostatic pressure (T/P_{HEL}).

$$D = \sum \frac{\Delta\varepsilon^p}{\varepsilon_f^p} \quad (4)$$

$$\varepsilon_f^p = D_1(P^* + T^*)^{D_2} \quad (5)$$

Expt.	d_p (μm)	v (km s^{-1})	projectile material	target material	target thickness (mm)	#
This work	800 -2000	4.59- 5.49	Al 2017, nylon, stainless steels 420, 304, 316, chrome steel 52100, cellulose acetate	soda-lime glass	25.4	30
Ref. 13	1100 - 2500	4.0 - 9.1	Al, Ti	Fused quartz	14.2	5
Ref. 14	397-1000	2.91-8.60	Al 2017, garnet	fused silica	14.2, 17.5	52
Ref. 15	550-800	1.0-7.5	pyrex, sapphire, tungsten carbide	fused silica	not known	12
Ref. 16	48	6-16.6	borosilicate glass	A/S glass, quartz	not known	53
Ref. 17	550-800	1.7 - 2.9	Al, Fe, Glass	granite, basalt, basalt glass	not known	13

Table 1. Parameters for the impact data used in this work (A/S : aluminosilicate glass)(#:number of shots)

The fracture damage is accumulated by summing the plastic strain during a cycle of integration, in a manner similar to that used in the Johnson-Cook fracture model. $\Delta\varepsilon^p$ is the plastic strain during a cycle of integration and ε_f^p is the plastic strain to fracture under constant P.

The Johnson-Holmquist 2 model was formulated with a polynomial equation of state which is energy independent. It also includes a term (ΔP) to describe bulking (Eq. 6). The incremental internal elastic energy decrease (due to decreased shear and deviator stresses) is converted to potential internal energy by incrementally increasing ΔP (Eq. 7). K1, K2 and K3 are material constants, obtained from fits to experimental data. β is the fraction of elastic material energy that is converted from elastic to hydrostatic energy ($0 \le \beta \le 1$). μ is the density increase in the material ($\mu=(\rho/\rho_0-1)$.

$$P=K1\mu+K2\mu^2+K3\mu^3+\Delta P \tag{6}$$

$$\Delta P_{t+\Delta t}=-K1\mu_{t+\Delta t}+\sqrt{(K1\mu_{t+\Delta t}+\Delta P_t)^2+2\beta K1\Delta U} \tag{7}$$

The JH-2 model constants (A, N, B, M, C, D_1, D_2) were obtained from flyer plate tests and ballistic long-rod penetration tests onto soda-lime glass at 1.5 - 2.4 km s^{-1} (Ref. 12).

3. EXPERIMENTAL DATA AND DAMAGE EQUATIONS

Validation of a hydrocode model can be carried out against experimentally produced data. If it is calibrated against laboratory data, it can be extrapolated with more confidence to a higher velocity. Hydrocodes can also be tested against power-law damage equations which are derived from laboratory data. These equations are frequently used to predict the damage sustained in the space environment at impact velocities not achievable in the laboratory.

In this section, we review two penetration equations (Eq. 8 from Ref. 16 and Eq. 9 from Ref. 18) against the experiment data in Table 1. The equations are tested for reproducibility of the data set, and checked for trends with velocity which might indicate that the parameters used are inaccurate. We also review the impact morphology for impacts onto finite soda-lime glass (Figure 1). The impact morphology has been noted in Ref. 8 to be different for impacts with $d_p > 300$ μm.

$$T_c=0.53d_p^{1.2}\rho_p^{0.5}v_p^{0.67} \tag{8}$$

$$T_c=0.53d_p^{1.06}\rho_p^{0.5}v_p^{0.67} \tag{9}$$

(T_c is depth of penetration (cm), d_p is the projectile diameter (cm), ρ_p is the projectile density (g cm^{-3}) and v_p is the velocity of the projectile (km s^{-1})).

A ratio R is defined such that R=(equation prediction)/(experimentally determined value) and is used to test the reproducibility of the equations. The average values and standard deviations of the equation predictions for each data set are given in Table 2.

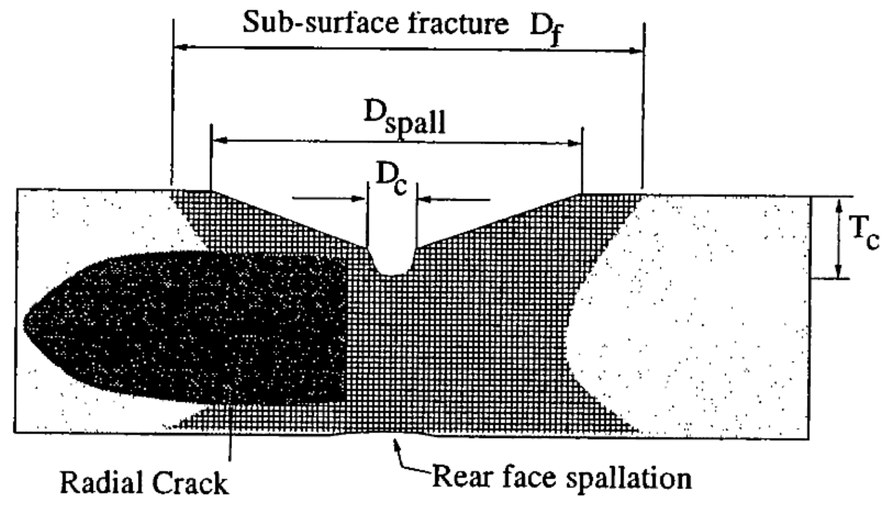

Fig. 1. Hypervelocity impact morphology

Experimenter	Eq. 8		Eq. 9	
	R (ave.)	R (st.)	R (ave.)	R (st.)
This work (semi-inf.)	0.99	0.21	1.33	0.27
This work (finite)	0.90	0.20	1.16	0.24
Ref. 13	0.92	0.25	1.20	0.36
Ref. 14 (semi-infinite)	0.48	0.11	0.76	0.17
Ref. 14 (finite)	0.70	0.24	1.01	0.33
Ref. 15	0.28	0.06	0.44	0.09
Ref. 16	1.19	0.27	2.52	0.58
Ref. 17	0.88	0.15	1.28	0.22

Table 2. Values of R for Table 1(ave: average, st. : standard deviation)

Variations in the target material type can be seen between, for instance, fused silica (Ref. 14) and soda-lime glass (this work). For most of the data sets, the equations predict the experimental values within ± 30 %. However, in figures 2 and 3, the data are plotted against velocity. The correlation between R and velocity implies that the values of the exponents in Eqs. 8 and 9 could be inaccurate. A random distribution of R about R=1 implies correct exponent values. This reduces confidence in the extrapolation of Eqs. 8 and 9 to higher velocities.

Most experimenters have recorded the depth (T_c) and the spallation diameter (D_{spall}) diameter but not the central crater diameter (D_c). In this shot programme, the crater profile (T_c/D_c) on the soda-lime glass was observed to be non-hemispherical and varying with density. Crater profiles are summarised in Table 3. Therefore, the crater profile cannot be extrapolated to the original crater surface unless the shape is quantitatively determined. The transient crater profile is lost when the front surface is spalled off (Fig 1). This limits the usefulness of D_c as a hydrocode calibration parameter.

Projectile	ρ (g cm^{-3})	T_c/D_c ave.	T_c/D_c (st.)	T_c/D_c (average measurement error)
Nylons	1.15 - 1.45	0.64	0.06	0.17
Al 2017	2.78	0.59	0.17	0.24
Ti / Ruby	4.0 - 4.5	0.75	0.21	0.17
Steels	7.75 - 8.47	0.81	0.20	0.21
Ref. 13 (Al)	2.8	0.75	0.26	n/a
Ref. 13 (Ti)	4.5	1.33	n/a	n/a

Table 3 : Crater profiles in soda-lime glass (this work and Ref. 13)

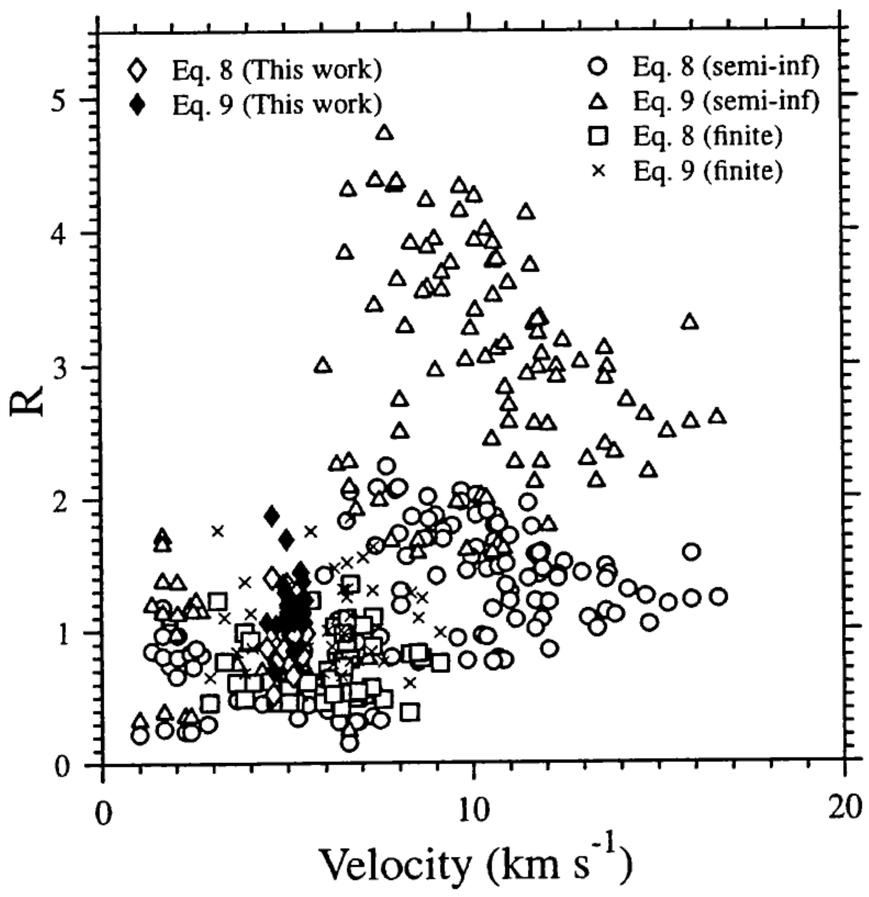

Fig. 2. Glass penetration equations compared to experimental data

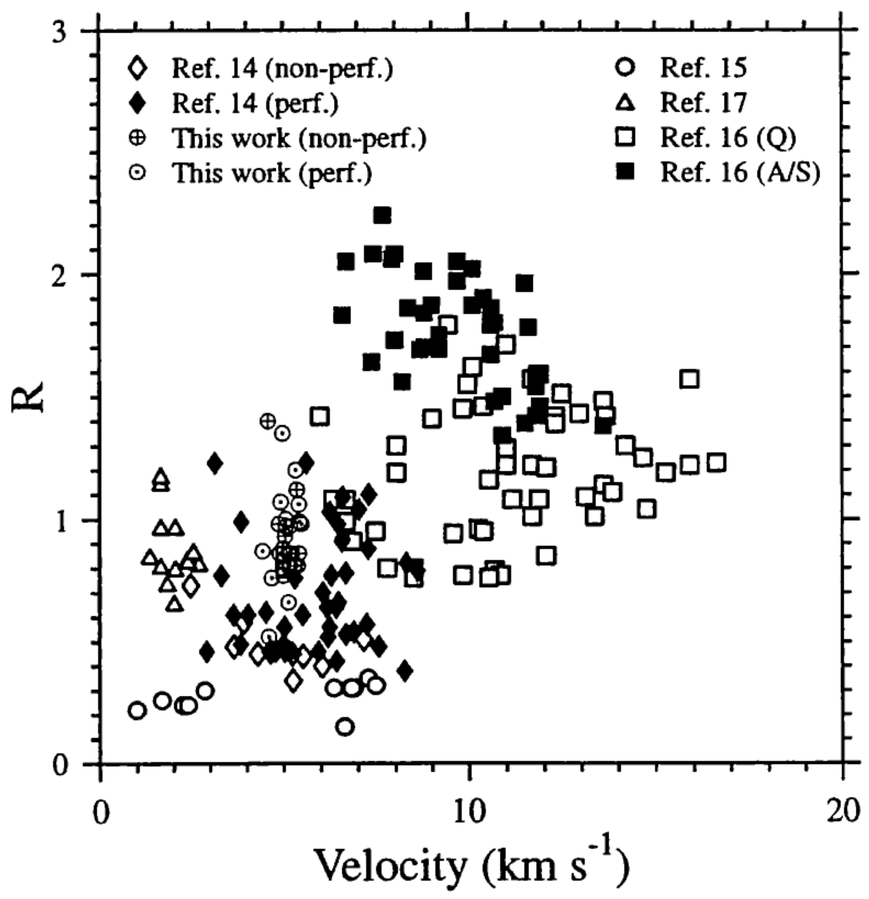

Fig.3. Eq. 8 : Target material dependence.

4. SIMULATION RESULTS

The Lagrangian simulations were run using the Johnson-Holmquist 2 model for glass. Dilation effects were included (β=1) but strain rate effects were not. 150 computational zones were used to define the target mesh. The simulations were run for a 1 mm Al projectile at impact velocities in the range of 5 to 15 km s^{-1}. The crater depth and diameter measurements are given in Table 4. In Figures 4 and 5, the damage and effective strain for JH 3012 and JH 3013 are presented. As discussed in section 3, comparison with experimental data has to be carried out with the following points in mind :

1. The velocity exponent in the damage equations (Eqs. 8 and 9) developed from experimental data may not accurately reflect the experimental data from which they were derived.
2. There is some evidence that material type is important in determining the depth of penetration.
3. The hydrocode D_c value cannot be accurately compared with the experimentally determined D_c value. The transient crater profile is lost when the front surface is spalled off (Fig. 1).

IDENT	Vel. (km s^{-1})	T_c (mm)	T_c (mm) (Eq. 8)	T_c (mm) (Eq. 9)
JH 3011	5	2.2	1.6	2.3
JH 3013	6	2.5	1.9	2.6
JH 3015	7	2.7	2.1	2.8
JH 3014	8	2.9	2.3	3.1
JH 3012	10	3.0	2.6	3.6
JH 3017	15	3.5	3.4	4.7

Table 4. Results from the Johnson-Holmquist 2 simulations in AUTODYN-2D

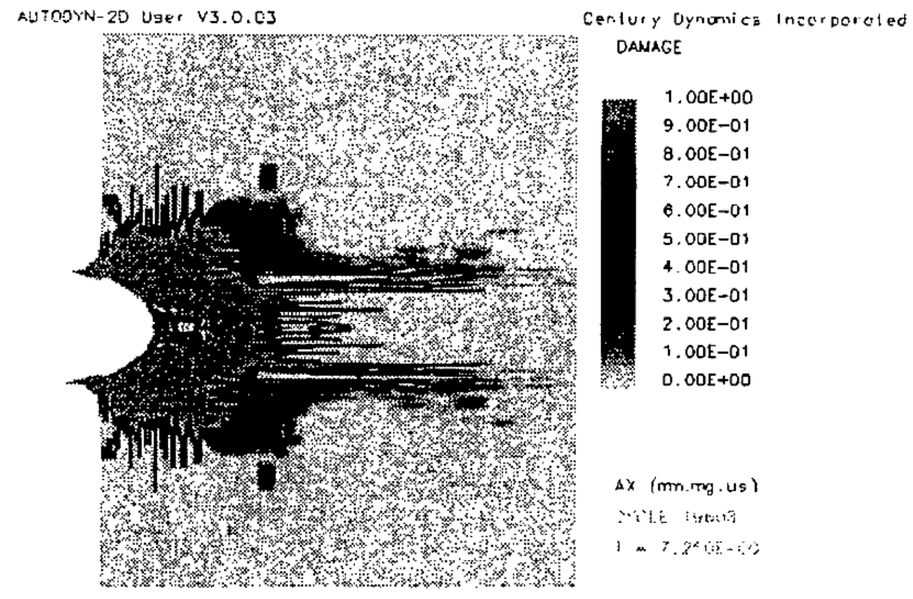

Fig 4. Damage for a 1mm Al impact onto Semi-Infinite Soda-Lime Glass at 6 km s^{-1} and 10 km s^{-1}

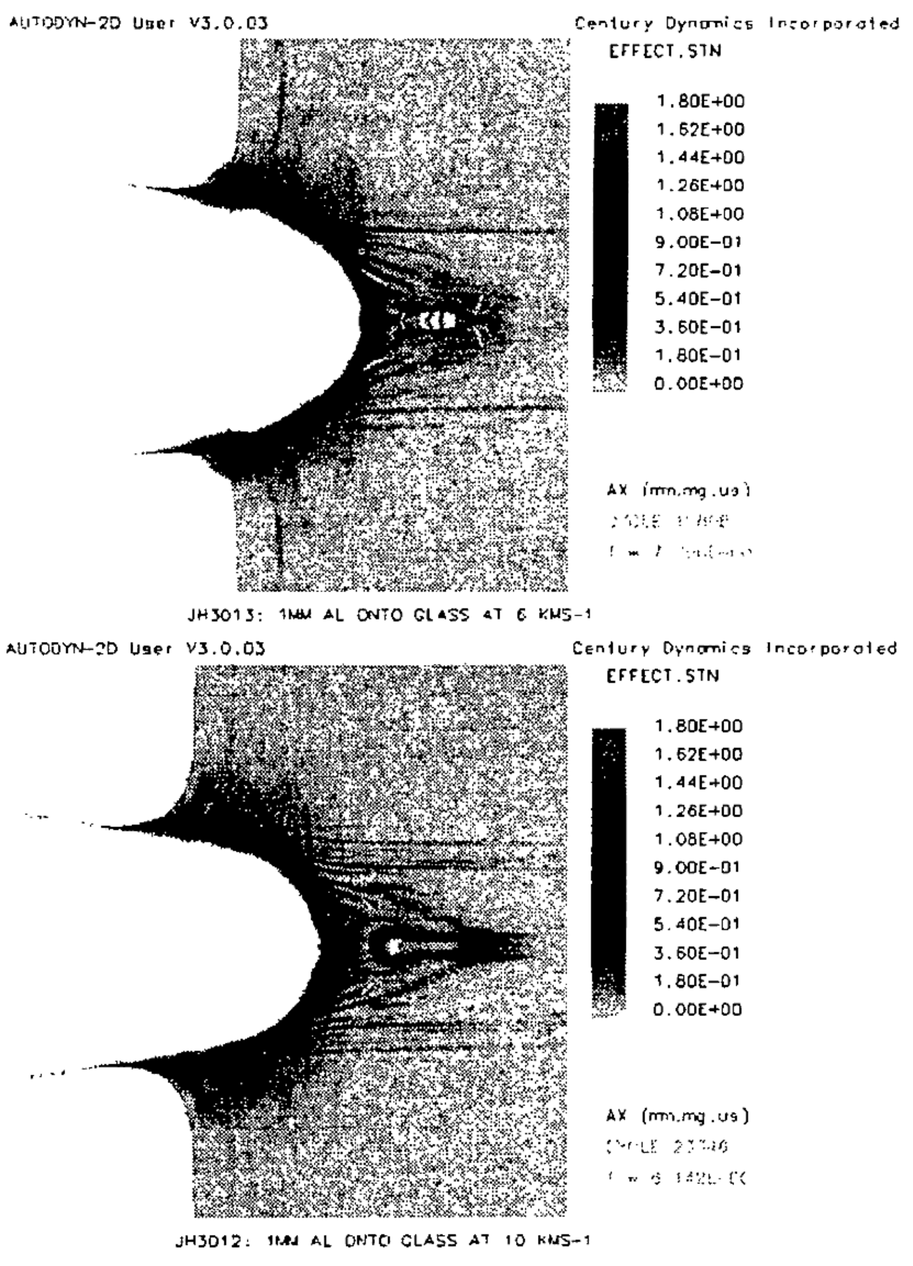

Fig. 5 . Effective Strain for a 1 mm Al impact onto Semi-Infinite Soda-Lime Glass at 6 km s^{-1} and 10 km s^{-1}

The results show that the hydrocode modelling values lie between the predictions of Eq. 8 and Eq. 9. For Eq. 8, R approaches the value 1 as the velocity increases whilst the opposite is true for Eq. 9 predictions.

Further development and validation of the Johnson-Holmquist soda-lime glass model, using experimentally derived damage equations, will not be possible until the damage equations have been adjusted. Development of a new damage equation is beyond the scope of this paper but will form part of further work.

5. DISCUSSION

The depth results presented in Table 4 show that the Johnson-Holmquist 2 model does reproduce the depth values predicted by two brittle material damage equations and the experimental data in the shot programme. However, the range of values predicted by the equation and experimental data cover a wide band. The crater values are not comparable with the experimentally measured values because the transient crater is spalled off. Modified parameters for the Johnson-Holmquist model can be derived from further flyer plate calibration tests (Ref. 19) and impact tests which are more comparable to the regimes being explored. The model itself requires modification to include an energy dependent term for modelling phase changes. More work needs to be done on the damage equations so as to be able to extrapolate to higher velocities with confidence.

6. CONCLUSION

The Johnson-Holmquist model is able to reproduce values of depth penetration produced in laboratory tests and predicted by experimentally determined damage equations for a 1 mm aluminium projectile impacting a semi-infinite target at 5-15 km s^{-1}. We were not able to reproduce crater or spallation diameters in this initial study, therefore crater diameters from experimental shots could not be used for calibration. Crater profiles were shown to vary with projectile density in the experimental shots. Limitations in the calibration data, derived from experimentally determined power-law equations, were identified which may be due to incorrect exponent values. The tentative conclusion is that the Johnson-Holmquist model is applicable to compressive regimes but does not appear to predict tensile fracture.

7. FUTURE WORK

An energy dependent model, derived by one of the authors (K. Tsembelis), will be implemented into the AUTODYN-2D code. Modified parameters for the model will be derived using recent shock wave data on soda-lime glass. The modelling of tensile fracture will be addressed in further studies by the authors. The influence of strain rate effects on the modelling results will be assessed as

well as the influence of thermal softening on the final crater shape.

8. ACKNOWLEDGEMENTS

E. A. Taylor would like to acknowledge financial support from Matra Marconi Space (UK), The Royal Academy of Engineering and the Royal Aeronautical Society.

9. REFERENCES

1. Johnson, G. R. and Holmquist, T. J., An Improved Computational Constitutive Model for Brittle Materials, Joint AIRA/APS Conference, Colorado Springs, Colorado, June 1993.
2. Birnbaum, N. K. et al., AUTODYN - An Interactive Non-Linear Dynamic Analysis Program for the Microcomputers through Supercomputers, *Proc. 9th International Conference on Structural Mechanics in Reactor Technology,* Lausanne, 1987.
3. Robertson, N. J., Hayhurst, C. J. and Fairlie, G., Numerical Simulation of Impact and Fast Transient Phenomena using AUTODYN-2D and 3D, *SMIRT IMPACT IV*, Berlin, Germany, August 1993.
4. McDonnell, J. A. M., Gardner, D. J., Newman, P. J., Robertson, N. J., Hayhurst, C. J., Hydrocode Modelling in the Study of Space Debris Impact Crater Morphology, *Proc. 1st Euro. Conf. on Space Debris*, Darmstadt, Germany, April 1993, SD-01.
5. Hayhurst, C. J., Ranson, H. J., Gardner, D. J., Birnbaum, N. K., Modelling of Microparticle Hypervelocity Oblique Impacts on Thick Targets, Int. J. Impact Engng., Vol. 17, pp. 375-386, 1995
6. Hayhurst, C. J. and Clegg, R. A., Cylindrically Symmetric SPH Simulations of Hypervelocity Impacts on Thin Plates, Int. J. Impact Engng., vol. 20 (to be published).
7. Shrine, N. R. G., Taylor, E. A., Griffiths, A. D., McDonnell, J. A. M., Using Solar Cells as Micro-Particle Detectors in Low Earth Orbit, presented at SPIE '96, Denver, 8-9 August 1996. *'Characteristics and Consequences of Orbital Debris and Natural Space Impactors'*, SPIE Proceedings 2813, pp. 76-87.
8. Taylor, E. A.. and McDonnell, J. A. M., Hypervelocity Impact On Soda Lime Glass: Damage Equations For Impactors In The 400-2000 μm Range, COSPAR '96, Birmingham, U.K., 14-21 July 1996. Accepted for publication in *Adv. Space Res.*
9. Alwes, D., Columbus-Viewport Glass Pane Hypervelocity Impact Testing and Analysis, Int. J. Impact Engng., Vl. 10, pp. 1-22, 1990.
10. McSherry, F., Numerical Simluations of Hypervelocity Impacts on Solar Arrays, ESA Contract No., 11693/95/NL/JG, 1996.
11. Medina, D. F., Serna, P. J., Allahdadi, F. A., Reconstruction of a Hypervelocity Impact Event in Space, presented at SPIE '96, Denver, 8-9 August 1996. *'Characteristics and Consequences of Orbital Debris and Natural Space Impactors'*, SPIE Proceedings 2813, pp. 137-147.
12. Holmquist, T. J., Johnson, G. R., Grady, D. E., Lopatin, C. M. and Hertel, E. S., Jr., High Strain Rate Properties and Constitutive Modeling of Glass, *15th Int. Symp. Ballistics*, Jerusalem, 21-24 May 1995.
13. Schneider, E., Stilp, A. J. and Kagerbauer, G., Meteoroid / Debris Simulation Experiments on MIR Viewport Samples, Int. J. Impact Engng., Vol. 17, pp. 731-737, 1995.
14. Edelstein, K.S., Hypervelocity Impact Damage Tolerance of Fused Silica, 43rd International Astronautical Congress, August 28 - September 5, 1992, Washington DC, IAF 92-0334 ,1992.
15. Flaherty, R. E., Impact Characteristics in Fused Silica, Conf. AIAA, 69-3647, 1969.
16. McHugh, A. H. and Richardson, A. J., Hypervelocity Particle Impact Damage to Glass, North American Aviation, STR-241, 1969.
17. Mandeville, J. C., unpublished data in, Berthoud, L. and Taylor, E. A., Analysis of Impact Calibration Tests (Work Package 2) : Interim report, ESA Contract AO 3053 Micrometeoroids and Debris Flux and Ejecta Models, August 1996.
18. Cour-Palais, B. G., Hypervelocity Impact Investigation and Meteoroid Shielding Experiments related to Apollo and Skylab, in *Orbital Debris*, CP-2360, 1982
19. Bourne, N. K., Rosenberg, Z, Mebar, Y., Obara, T and Field, J. E., A High Speed Photographic Study of Fracture Wave Propagation in Glasses, J. de Phys. IV, Coll. C8, C8-635-640, 1994.